

Exploring bottom-charmed molecular tetraquarks with complex scaling method

Qing-Fu Song,^{1,*} Wei Liang,¹ Qi-Fang Lü,^{2,3,4,†} and Xiao-Nu Xiong^{1,‡}

¹*School of Physics, Central South University, Changsha 410083, China*

²*Department of Physics, Hunan Normal University, Changsha 410081, China*

³*Key Laboratory of Low-Dimensional Quantum Structures and Quantum Control of Ministry of Education, Changsha 410081, China*

⁴*Key Laboratory for Matter Microstructure and Function of Hunan Province, Hunan Normal University, Changsha 410081, China*

In this work, we analyze the $D_{(s)}^{(*)}B_{(s)}^{(*)}$ interactions by adopting the one boson exchange model from a coupled channel perspective. For $I(J^P) = 1(1^+) DB^*/D^*B/D^*B^*$ system, utilizing the complex scaling method, we obtain a loosely bound state and two resonant states below DB^* , D^*B , and D^*B^* thresholds, respectively. Assuming that charmonium-like states $T_{c\bar{c}1}(3900)$, $T_{c\bar{c}1}(4020)$ and bottomonium-like states $T_{b\bar{b}1}(10610)$, $T_{b\bar{b}1}(10650)$ are molecular states near the corresponding thresholds, we suggest these predicted particles in $I(J^P) = 1(1^+)$ system as their analogues. In addition, we extend our study to other $D_{(s)}^{(*)}B_{(s)}^{(*)}$ combinations with different quantum numbers. According to our estimations, there may exist some exotic structures in bottom-charmed sector. Finally, we collect the possible decay channels for future experimental observations. The B_c/B_c^* plus a light meson are the ideal final state to search for the bound states, while the $D_{(s)}^{(*)}B_{(s)}^{(*)}$ channels are suitable for the resonances. We highly recommend that the future experiments hunt for these bottom-charmed exotic particles.

Keywords: bottom-charmed, molecular states, coupled channel analysis, complex scaling method

I. INTRODUCTION

The discovery of hidden charm state $X(3872)$ with $J^{PC} = 1^{++}$ in the process $B^\pm \rightarrow K^\pm \pi^+ \pi^- J/\psi$ by the Belle Collaboration in 2003 caused a series of interesting consequences for the establishment of hadronic spectra [1]. Since $X(3872)$ lies very close to the $D\bar{D}^* + h.c.$ threshold, it was naturally interpreted as a $D\bar{D}^*$ hadronic molecular state. This discovery sparks further interest in exotic hadrons, especially in the charm sector. In 2013, the BESIII [2] and Belle [3] Collaborations observed a charged charmonium-like state named $T_{c\bar{c}1}(3900)$, which generates even more attention. As $T_{c\bar{c}1}(3900)$ is located slightly above the $D\bar{D}^* + h.c.$ threshold, it can be identified as the isospin partner of $X(3872)$. According to heavy quark spin symmetry, there should exist charmonium-like states in $D^*\bar{D}^*$ channel. Indeed, an isovector state $T_{c\bar{c}1}(4020)$ and an isoscalar state $X(4013)$ were subsequently discovered by the BESIII [4] and Belle [5] Collaborations, respectively. Meanwhile, for the bottom sector, two bottomonium-like states $T_{c\bar{c}1}(10610)$ and $T_{c\bar{c}1}(10650)$ were reported by the Belle Collaboration in 2011 [6]. These states with $I(J^{PC}) = 1(1^{+-})$ have masses of $10607.2^{+2.2}_{-2.2}$ and $10652.2^{+1.5}_{-1.5}$ MeV, and widths of $18.4^{+2.4}_{-2.4}$ and $11.5^{+2.2}_{-2.2}$ MeV, respectively. These findings provide additional evidence for the existence of exotic hadrons in both the charm and bottom sectors. Meanwhile, a series of new phenomenological studies on the XYZ and P_c/T_{cc} states have been reported in references [7–23].

The B_c meson was first observed in 1998 by the CDF Collaboration through the decay modes $B_c^\pm \rightarrow J/\psi \ell^\pm X$ and $B_c^\pm \rightarrow J/\psi \ell^\pm \bar{\nu}_\ell$ in $p\bar{p}$ collisions, with a mass measurement of $6.40 \pm 0.39 \pm 0.13 \text{ GeV}$ [24], which was confirmed by

the LHCb and D0 Collaborations later [25, 26]. According to Particle Data Group (PDG) [27], it has a mass of $m = 6274.47 \pm 0.32 \text{ MeV}$ and with $I(J^P) = 0(0^-)$. In 2019, the CMS Collaboration reported the discovery of radially excited states $B_c^+(2^1S_0)$ and $B_c^{*+}(2^3S_1)$ in the $B_c^+ \pi^+ \pi^-$ invariant mass spectrum, and these two states have a mass difference $m(2^1S_0) - m(2^3S_1) = 29 \pm 1.5 \pm 0.7 \text{ MeV}$ [28]. In the same year, the LHCb Collaboration also observed two excited $\bar{c}b$ states in the same decay channel. The masses of these two states were measured to be $6841.2 \pm 0.6 \pm 0.1 \pm 0.8 \text{ MeV}$ and $6872.1 \pm 1.3 \pm 0.1 \pm 0.8 \text{ MeV}$, respectively [29]. However, until now, there are no more significant experimental signals for hadrons containing both charm and bottom quarks, which include conventional mesons and tetraquarks.

In theory, the spectroscopy of traditional bottom-charmed meson was extensively discussed in references in the framework of quark models [30–43], lattice QCD [44–46], and QCD sum rules [47, 48]. The bottom-charmed molecular tetraquarks, named as B_c -like states, have not been observed in experiments, the first principles of quantum chromodynamics (QCD) do not prohibit their existence. Theoretically, there are plenty of works that focus on their existences and properties. In Ref. [49], the author calculated the mass spectra of $cq\bar{b}\bar{q}$, $cs\bar{b}\bar{q}$, and $cs\bar{b}\bar{s}$ components using the chromomagnetic interaction model. Within the QCD sum rules method and QCD light-cone sum rules, many references extensively investigate the properties of B_c -like states [50–58]. For instance, in Ref. [58], the authors examined the masses of $Q\bar{q}\bar{Q}^{(\prime)}q$ molecules and obtained some bound states in the QCD sum rules framework for the bottom-charmed sector. The chiral unitary approach and the hidden gauge symmetry Lagrangians have also been employed to study B_c -like molecular states [59, 60]. Additionally, in Ref. [61], the interaction of $B_{(s)}^{(*)}$ and $D_{(s)}^{(*)}$ mesons was studied by applying one boson exchange (OBE) model, and their results showed that there may exist some molecular states. Also, in Ref. [62], the authors perform a study on radiative decays and magnetic moments for bottom-charmed molecular tetraquarks.

*Electronic address: 242201003@csu.edu.cn

†Electronic address: lvqifang@hunnu.edu.cn

‡Electronic address: nxniong@csu.edu.cn

Charmed Sector	Bottom Charmed Sector	Bottom Sector
$D^* \bar{D}^*$ $T_{c\bar{c}1}(4020), X(4014)$	$D^* B^*$ $T_{c\bar{b}1}, X(?)$	$B^* \bar{B}^*$ $T_{b\bar{b}1}(10650), X(?)$
$D \bar{D}^*$ $T_{c\bar{c}1}(3900), X(3872)$	$DB^* \text{ or } D^* B$ $T_{c\bar{b}1}, X(?)$	$B \bar{B}^*$ $T_{b\bar{b}1}(10610), X(?)$

FIG. 1: Comparison of $J^P = 1^+$ states for charmed, bottom-charmed, and bottom sectors.

However, it is far away from establishing the complete spectroscopy for B_c -like molecular tetraquark states, our understanding of them is still scarce. The explorations of bottom-charmed molecular tetraquark states may provide new insights into the nature of the exotic states observed near the $D^{(*)}\bar{D}^*$ and $B^{(*)}\bar{B}^*$ thresholds. On the other hand, the heavy quark symmetry (HQS) implies that the strong interaction dynamics for heavy quarks should be similar regardless of whether the quark is a charm or bottom quark. As illustrated in Figure 1, the HQS allows the existence of exotic hadronic states in the bottom-charmed sector, which are expected to be counterparts to the exotic states already observed in both the charm and bottom sectors. Furthermore, coupled channel effects and $S - D$ wave mixing effects are expected to play an important role in the production of these molecular states. Thus, it is urgent to study the $D_{(s)}^{(*)}B_{(s)}^{(*)}$ systems systematically with the coupled channel approach and explore some possible excited resonances together with bound states.

Recently, we systematically have explore the properties of the hidden bottom molecular tetraquarks and the bottom-strange molecular pentaquarks by adopting the one boson exchange model [63, 64]. Utilizing the Gaussian expansion method [65, 66] and complex scaling method [67, 68], the coupled-channel Schrödinger equation is solved in order to obtain poles. In the present work, performing the same procedure, we systematically investigate bottom-charmed molecular tetraquark states. Firstly, we investigate $DB^*/D^*B/D^*B^*$ with $I(J^P) = 1(1^+)$, which helps to determine the free parameter cutoff Λ . According to our estimations, we predict a bound state below DB^* channel, and two resonances lie below D^*B and D^*B^* thresholds, respectively. Then, we extend our explorations to others various $D_{(s)}^{(*)}B_{(s)}^{(*)}$ with different quantum numbers. In short, we predict three molecular states for $I(J^P) = 0(0^+)$ system, one for $I(J^P) = 0(1^+)$ system, one for $I(J^P) = 0(2^+)$ system, one for $I(J^P) = 1(0^+)$ system, and three for $I(J^P) = 1(1^+)$ system. We hope that our predictions can offer some useful information for future experiments observa-

tions.

This paper is organized as follows. The formalism of effective interactions and complex scaling method are briefly introduced in Sec. II. We present the numerical results and discussions for the $D_{(s)}^{(*)}B_{(s)}^{(*)}$ systems in Sec. III. A summary is given in the last section.

II. FORMALISM

A. The effective interactions

In the present work, we employ the OBE model to obtain the effective potential of the $D_{(s)}^{(*)}B_{(s)}^{(*)}$ systems. The OBE model describes meson-meson interaction by exchanging the light scalar, pseudoscalar and vector mesons, which is successfully applied to explain the dynamic mechanisms of molecular states. Under the heavy quark symmetry and chiral symmetry, the relevant effective Lagrangians can be expressed as [69–72]

$$\begin{aligned} \mathcal{L} = & g_\sigma \left\langle H_a^{(\mathcal{Q})} \sigma \bar{H}_a^{(\mathcal{Q})} \right\rangle + g_\sigma \left\langle \bar{H}_a^{(\mathcal{Q})} \sigma H_a^{(\mathcal{Q})} \right\rangle \\ & + ig \left\langle H_b^{(\mathcal{Q})} \mathcal{A}_{ba} \gamma_5 \bar{H}_a^{(\mathcal{Q})} \right\rangle + ig \left\langle \bar{H}_a^{(\mathcal{Q})} \mathcal{A}_{ab} \gamma_5 H_b^{(\mathcal{Q})} \right\rangle \\ & + \left\langle i H_b^{(\mathcal{Q})} \left(\beta v^\mu (\mathcal{V}_\mu - \rho_\mu) + \lambda \sigma^{\mu\nu} F_{\mu\nu}(\rho) \right)_{ba} \bar{H}_a^{(\mathcal{Q})} \right\rangle \\ & - \left\langle i \bar{H}_a^{(\mathcal{Q})} \left(\beta v^\mu (\mathcal{V}_\mu - \rho_\mu) - \lambda \sigma^{\mu\nu} F_{\mu\nu}(\rho) \right)_{ab} H_b^{(\mathcal{Q})} \right\rangle, \end{aligned} \quad (1)$$

where a and b is the flavor indices, and $v^\mu = (1, \mathbf{0})$ is the four-velocity. The vector current is

$$\mathcal{V}_\mu = \frac{1}{2} (\xi^\dagger \partial_\mu \xi + \xi \partial_\mu \xi^\dagger), \quad (2)$$

the axial current is

$$A_\mu = \frac{1}{2} (\xi^\dagger \partial_\mu \xi - \xi \partial_\mu \xi^\dagger), \quad (3)$$

and strength tensor of vector field is

$$F_{\mu\nu}(\rho) = \partial_\mu \rho_\nu - \partial_\nu \rho_\mu + [\rho_\mu, \rho_\nu], \quad (4)$$

where $\xi = \exp(i\mathbb{P}/f_\pi)$ and $\rho_\mu = ig_V \mathcal{V}_\mu / \sqrt{2}$. The $f_\pi = 132$ MeV is the pion decay constant, and then $g_V = m_\rho / f_\pi = 5.8$ [73]. The \mathbb{P} and \mathbb{V} stand for the matrices of light pseudoscalar and vector mesons, respectively,

$$\begin{aligned} \mathbb{P} &= \begin{pmatrix} \frac{\pi^0}{\sqrt{2}} + \frac{\eta}{\sqrt{6}} & \pi^+ & K^+ \\ \pi^- & -\frac{\pi^0}{\sqrt{2}} + \frac{\eta}{\sqrt{6}} & K^0 \\ K^- & \bar{K}^0 & -\sqrt{\frac{2}{3}}\eta \end{pmatrix}, \\ \mathbb{V} &= \begin{pmatrix} \frac{\rho^0}{\sqrt{2}} + \frac{\omega}{\sqrt{2}} & \rho^+ & K^{*+} \\ \rho^- & -\frac{\rho^0}{\sqrt{2}} + \frac{\omega}{\sqrt{2}} & K^{*0} \\ K^{*-} & \bar{K}^{*0} & \phi \end{pmatrix}. \end{aligned} \quad (5)$$

The $H_a^{(Q)}$, $H_a^{(\bar{Q})}$, $\bar{H}_a^{(Q)}$, and $\bar{H}_a^{(\bar{Q})}$ represent the fields of heavy-light mesons and can be written as

$$H_a^{(Q)} = (1 + \not{p})(\mathcal{P}_a^{*(Q)\mu}\gamma_\mu - \mathcal{P}_a^{(Q)}\gamma_5)/2, \quad (6)$$

$$H_a^{(\bar{Q})} = (\bar{\mathcal{P}}_a^{*(\bar{Q})\mu}\gamma_\mu - \bar{\mathcal{P}}_a^{(\bar{Q})}\gamma_5)(1 - \not{p})/2, \quad (7)$$

$$\bar{H} = \gamma_0 H^\dagger \gamma_0. \quad (8)$$

More explicitly, the effective Lagrangian depicting the couplings of light mesons and heavy-light mesons can be written as [74–76]

$$\mathcal{L}_{\mathcal{P}\mathcal{P}\mathbb{V}} = -\sqrt{2}\beta g_V \mathcal{P}_b \mathcal{P}_a^\dagger \cdot \mathbb{V}_{ba} + \sqrt{2}\beta g_V \tilde{\mathcal{P}}_b^\dagger \tilde{\mathcal{P}}_a \cdot \mathbb{V}_{ab}, \quad (9)$$

$$\begin{aligned} \mathcal{L}_{\mathcal{P}^*\mathcal{P}\mathbb{V}} &= -2\sqrt{2}\lambda g_V \mathbb{V}^\lambda \varepsilon_{\lambda\mu\alpha\beta} (\mathcal{P}_b \mathcal{P}_a^{*\mu\dagger} + \mathcal{P}_b^{*\mu} \mathcal{P}_a^\dagger) (\partial^\alpha \mathbb{V}^\beta)_{ba} \\ &\quad - 2\sqrt{2}\lambda g_V \mathbb{V}^\lambda \varepsilon_{\lambda\mu\alpha\beta} (\tilde{\mathcal{P}}_b^{*\mu\dagger} \tilde{\mathcal{P}}_a + \tilde{\mathcal{P}}_b^\dagger \tilde{\mathcal{P}}_a^{*\mu}) (\partial^\alpha \mathbb{V}^\beta)_{ab}, \end{aligned} \quad (10)$$

$$\begin{aligned} \mathcal{L}_{\mathcal{P}^*\mathcal{P}^*\mathbb{V}} &= \sqrt{2}\beta g_V \mathcal{P}_b^* \cdot \mathcal{P}_a^{*\dagger} \cdot \mathbb{V}_{ba} \\ &\quad - i2\sqrt{2}\lambda g_V \mathcal{P}_b^{*\mu} \mathcal{P}_a^{*\nu\dagger} (\partial_\mu \mathbb{V}_\nu - \partial_\nu \mathbb{V}_\mu)_{ba} \\ &\quad - \sqrt{2}\beta g_V \tilde{\mathcal{P}}_b^{*\mu\dagger} \tilde{\mathcal{P}}_a^{*\nu} \cdot \mathbb{V}_{ab} \\ &\quad - i2\sqrt{2}\lambda g_V \tilde{\mathcal{P}}_b^{*\mu\dagger} \tilde{\mathcal{P}}_a^{*\nu} (\partial_\mu \mathbb{V}_\nu - \partial_\nu \mathbb{V}_\mu)_{ab}, \end{aligned} \quad (11)$$

$$\begin{aligned} \mathcal{L}_{\mathcal{P}^*\mathcal{P}^*\mathbb{P}} &= -i\frac{2g}{f_\pi} \mathbb{V}^\beta \varepsilon_{\beta\mu\alpha\nu} \mathcal{P}_b^{*\mu} \mathcal{P}_a^{*\nu\dagger} \partial^\alpha \mathbb{P}_{ba} \\ &\quad + i\frac{2g}{f_\pi} \mathbb{V}^\beta \varepsilon_{\beta\mu\alpha\nu} \tilde{\mathcal{P}}_b^{*\mu\dagger} \tilde{\mathcal{P}}_a^{*\nu} \partial^\alpha \mathbb{P}_{ab}, \end{aligned} \quad (12)$$

$$\mathcal{L}_{\mathcal{P}\mathcal{P}\sigma} = -2g_s \mathcal{P}_b \mathcal{P}_b^\dagger \sigma - 2g_s \tilde{\mathcal{P}}_b \tilde{\mathcal{P}}_b^\dagger \sigma, \quad (13)$$

$$\mathcal{L}_{\mathcal{P}^*\mathcal{P}^*\sigma} = 2g_s \mathcal{P}_b^* \cdot \mathcal{P}_b^{*\dagger} \sigma + 2g_s \tilde{\mathcal{P}}_b^* \cdot \tilde{\mathcal{P}}_b^{*\dagger} \sigma, \quad (14)$$

where the relevant parameters and details can be found in Refs. [75, 77].

Using the given Lagrangians, we can deduce the relevant interaction potentials of these investigated systems in the momentum space straightforwardly. Based on the Breit approximation, the effective potential reads

$$\mathcal{V}^{M_1 M_2 \rightarrow M_3 M_4}(q) = -\frac{\mathcal{M}(M_1 M_2 \rightarrow M_3 M_4)}{4\sqrt{m_1 m_2 m_3 m_4}}, \quad (15)$$

where $\mathcal{M}(M_1 M_2 \rightarrow M_3 M_4)$ denotes the scattering amplitude for the $\mathcal{M}(M_1 M_2 \rightarrow M_3 M_4)$ process, and m_i is the mass of the meson M_i . One can obtain the final effective potential in position space after performing the Fourier transformation

$$\mathcal{V}(\mathbf{r}) = \int \frac{d^3 \mathbf{q}}{(2\pi)^3} e^{i\mathbf{q}\cdot\mathbf{r}} \mathcal{V}(\mathbf{q}) \mathcal{F}^2(q^2, m_i^2), \quad (16)$$

$$\mathcal{F}(q^2, m_i^2) = (\Lambda^2 - m_i^2)/(\Lambda^2 - q^2), \quad (17)$$

since the hadrons are not point particles, the form factor with the cutoff parameter Λ is introduced to account for the inner structures of them. Then, we can obtain the flavor-independent sub-potentials

$$\begin{aligned} V_v^a &= -\frac{1}{2}\beta^2 g_V^2 Y(\Lambda, m_v, r), \\ V_\sigma^a &= -g_s^2 Y(\Lambda, m_\sigma, r), \end{aligned} \quad (18)$$

for $PP \rightarrow PP$ process,

$$\begin{aligned} V_p^c &= -\frac{1}{3}\frac{g^2}{f_\pi^2} \mathcal{Z}_{\Lambda, m_p}, \\ V_v^c &= \frac{2}{3}\lambda^2 g_V^2 \mathcal{Z}'_{\Lambda, m_v}, \end{aligned} \quad (19)$$

for $PP \rightarrow P^*P^*$ process,

$$\begin{aligned} V_\sigma^d &= -g_s^2 \mathcal{Y}_{\Lambda, m_\sigma}, \\ V_v^d &= -\frac{1}{2}\beta^2 g_V^2 \mathcal{Y}_{\Lambda, m_v}, \end{aligned} \quad (20)$$

for $PP^* \rightarrow PP^*$ process,

$$\begin{aligned} V_p^e &= -\frac{1}{3}\frac{g^2}{f_\pi^2} \mathcal{Z}_{\Lambda, m_p}, \\ V_v^e &= \frac{2}{3}\lambda^2 g_V^2 \mathcal{Z}'_{\Lambda, m_v}, \end{aligned} \quad (21)$$

for $PP^* \rightarrow P^*P$ process, and

$$\begin{aligned} V_p^f &= -\frac{1}{3}\frac{g^2}{f_\pi^2} \mathcal{Z}_{\Lambda_i, m_i}^{ij}, \\ V_v^f &= \frac{2}{3}\lambda^2 g_V^2 \mathcal{X}_{\Lambda_i, m_i}^{ij}, \end{aligned} \quad (22)$$

for $PP^* \rightarrow P^*P^*$ process.

$$\begin{aligned} V_p^g &= -\frac{1}{3}\frac{g^2}{f_\pi^2} \mathcal{Z}_{\Lambda_i, m_i}^{ji}, \\ V_v^g &= \frac{2}{3}\lambda^2 g_V^2 \mathcal{X}_{\Lambda_i, m_i}^{ji}, \end{aligned} \quad (23)$$

for $P^*P \rightarrow P^*P^*$ process,

$$\begin{aligned} V_p^h &= -\frac{1}{3}\frac{g^2}{f_\pi^2} \mathcal{Z}_{\Lambda, m_p}, \\ V_\sigma^h &= -g_s^2 \mathcal{Y}_{\Lambda, m_\sigma}, \\ V_v^h &= -\frac{1}{2}\beta^2 g_V^2 \mathcal{Y}_{\Lambda, m_v} + \frac{2}{3}\lambda^2 g_V^2 \mathcal{Z}'_{\Lambda, m_v}, \end{aligned} \quad (24)$$

for $P^*P^* \rightarrow P^*P^*$ process. Some explicit formulas for the potentials can be expressed as

$$\begin{aligned} \mathcal{Z}_{\Lambda, m_a}^{ij} &= \left(\mathcal{E}_{ij} \nabla^2 + \mathcal{F}_{ij} r \frac{\partial}{\partial r} \frac{1}{r} \frac{\partial}{\partial r} \right) Y(\Lambda, m, r), \\ \mathcal{Z}'_{\Lambda, m_a}{}^{ij} &= \left(2\mathcal{E}_{ij} \nabla^2 - \mathcal{F}_{ij} r \frac{\partial}{\partial r} \frac{1}{r} \frac{\partial}{\partial r} \right) Y(\Lambda, m, r), \\ \mathcal{X}_{\Lambda, m_a}^{ij} &= \left(-2\mathcal{E}_{ij} \nabla^2 - (\mathcal{F}'_{ij} - \mathcal{F}''_{ij}) r \frac{\partial}{\partial r} \frac{1}{r} \frac{\partial}{\partial r} \right) Y(\Lambda, m, r), \\ \mathcal{Y}_{\Lambda, m_a}^{ij} &= \mathcal{D}_{ij} Y(\Lambda, m, r), \\ Y(\Lambda, m, r) &= \frac{1}{4\pi r} (e^{-mr} - e^{-\Lambda r}) - \frac{\Lambda^2 - m^2}{8\pi \Lambda} e^{-\Lambda r}. \end{aligned} \quad (25)$$

Here, \mathcal{D}_{ij} , \mathcal{E}_{ij} , and \mathcal{F}_{ij} represent the operators for spin-spin coupling and the tensor forces and relate with polarization

vector ϵ_i and Pauli matrix σ , respectively. Finally, the total effective potentials for $D_{(s)}^{(*)}B_{(s)}^{(*)}$ systems can be expressed by the combinations of these sub-potentials [74–76] and summarized in Table I. Also, the relevant parameters are collected in Table II [73, 75, 78–80].

B. Numerical solution methods

In this work, we use the Gaussian expansion method (GEM) to solve the coupled-channel Schrödinger equation, which is widely applied to solve the problem of a few-body system [65, 66]. In the GEM, the orbital wave functions are expanded in terms of a set of Gaussian basis functions

$$\phi_n(\mathbf{r}) = N_{nlr} r^{l_r} e^{-v_n r^2} Y_{l_r m_{l_r}}(\hat{\mathbf{r}}), \quad (26)$$

$$v_n = 1/r_n^2, r_n = r_1 a^{n-1} (n = 1, \dots, n_{max}), \quad (27)$$

where the Gaussian parameters $\{r_1, r_{max}, n_{max}\} = \{0.5 \text{ fm}, 25 \text{ fm}, 25\}$ are applied in the present work. In order to obtain resonance, the complex scaling method (CSM) is introduced. In the CSM, the Hamiltonian \hat{H} and wave function $|\Phi\rangle$ are transformed with complex rotation operator $\hat{U}(\theta)$

$$\hat{H}_\theta = \hat{U}(\theta) \hat{H} \hat{U}^{-1}(\theta), |\Phi_\theta\rangle = \hat{U}(\theta) |\Phi\rangle. \quad (28)$$

The coordinate \mathbf{r} and conjugate momentum \mathbf{p} are transformed to be

$$\mathbf{r} \rightarrow \mathbf{r} e^{i\theta}, \mathbf{p} \rightarrow \mathbf{p} e^{-i\theta}, \quad (29)$$

where the θ is variable and called scaling angle. Correspondingly, the complex scaling Schrödinger equation can be written as

$$\begin{pmatrix} e^{-2i\theta} T_{11} + V_{11}(re^{i\theta}) + W_1 & V_{12}(re^{i\theta}) & \dots & V_{1j}(re^{i\theta}) \\ V_{21}(re^{i\theta}) & e^{-2i\theta} T_{22} + V_{22}(re^{i\theta}) + W_2 & \dots & V_{2j}(re^{i\theta}) \\ \vdots & \vdots & \ddots & \vdots \\ V_{j1}(re^{i\theta}) & V_{j2}(re^{i\theta}) & \dots & e^{-2i\theta} T_{jj} + V_{jj}(re^{i\theta}) + W_j \end{pmatrix} \cdot \begin{pmatrix} \psi_1(r) \\ \psi_2(r) \\ \vdots \\ \psi_j(r) \end{pmatrix} = E \begin{pmatrix} \psi_1(r) \\ \psi_2(r) \\ \vdots \\ \psi_j(r) \end{pmatrix}.$$

The operator T_{ij} is defined as

$$T_{ij} = \frac{1}{2\mu_i} \left(-\frac{d^2}{dr^2} + \frac{l_i(l_i + 1)}{r^2} \right), \quad (30)$$

where W_{ij} represents the corresponding threshold. On the complex-energy plane, the eigenvalues of the scattering continuum states align along the so-called 2θ line, which satisfies the relation $1/2\text{Arg}(\Gamma/2E)$. In contrast, bound states and resonances remain independent of the scaling angle θ . This property allows one to distinguish bound states and resonances from the continuum states.

For a resonance, the RMS radius r_{RMS} and the composed proportion P are given by the c-product [81, 82]

$$r_{RMS}^2 = (\psi^\theta | r^2 | \psi^\theta) = \sum_i \int r^2 \psi_i^\theta(\mathbf{r})^2 d^3\mathbf{r},$$

$$P = (\psi_i^\theta | \psi_i^\theta) = \int \psi_i^\theta(\mathbf{r})^2 d^3\mathbf{r}, \quad (31)$$

where the ψ_i is the wave function of the i -th channel and obeys the normalization condition

$$\sum_i (\psi_i^\theta | \psi_i^\theta) = 1. \quad (32)$$

III. RESULTS AND DISCUSSIONS

A. Isospin vector systems

Performing above the procedures, one can explore the possible bound states and resonances of the $D_{(s)}^{(*)}B_{(s)}^{(*)}$ systems with various combinations by solving the coupled-channel Schrödinger equation with complex scaling method. In this work, the only free parameter is the UV cutoff Λ in Eq. (17), which reflects the internal structure of the interacting hadrons and may vary for different coupled systems and it lies within the range of 800 ~ 5000 MeV. A reasonable cutoff for deuteron studies is estimated to be around 1000 MeV, but it can also vary among different scenarios [83, 84]. It is important to note that in Ref. [75], the authors investigated the $D_{(s)}^{(*)}\bar{D}_{(s)}^{(*)}$ interactions, revealing charmonium-like resonances with quantum numbers $I(J^{PC}) = 0(0^{++})$ and $0(1^{+-})$ at cutoff values 1000 ~ 2000 MeV, where the poles are obtained at around 1500 MeV. In our previous work [63], we predicted several exotic hadron states for the $B_{(s)}^{(*)}\bar{B}_{(s)}^{(*)}$ systems by varying the cutoff in the range 800 ~ 1200 MeV. Since the interaction potential between the mesons is similar, the heavier mesons effectively reduce the contribution from the kinetic energy. Consequently, the cutoff value for the $D_{(s)}^{(*)}B_{(s)}^{(*)}$ systems is expected to lie between that of the $B_{(s)}^{(*)}\bar{B}_{(s)}^{(*)}$ systems and the $D_{(s)}^{(*)}\bar{D}_{(s)}^{(*)}$ systems. According to heavy quark sym-

TABLE I: The effective potentials for $D_{(s)}^{(*)}B_{(s)}^{(*)}$ systems.

$I(J^{PC}) = 0(0^+)$	DB	$D_s B_s$	$D^* B^*$	$D_s^* B_s^*$		
DB	$V_\sigma^a + \frac{3}{2}V_\rho^a + \frac{1}{2}V_\omega^a$	$\sqrt{2}V_{K^*}^a$	$\frac{1}{6}V_\eta^b + \frac{3}{2}V_\pi^b + \frac{3}{2}V_\rho^b + \frac{1}{2}V_\omega^b$	$\sqrt{2}V_{K^*}^b + \sqrt{2}V_K^b$		
$D_s B_s$		$V_\sigma^a + V_\phi^a$	$\sqrt{2}V_{K^*}^b + \sqrt{2}V_K^b$	$\frac{2}{3}V_\eta^b + V_\phi^b$		
$D^* B^*$			$V_\sigma^c + \frac{3}{2}V_\pi^c + \frac{1}{6}V_\eta^c + \frac{3}{2}V_\rho^c + \frac{1}{2}V_\omega^c$	$\sqrt{2}V_{K^*}^c + \sqrt{2}V_K^c$		
$D_s^* B_s^*$				$V_\sigma^c + \frac{2}{3}V_\eta^c + V_\phi^c$		
$I(J^{PC}) = 0(1^+)$	DB^*	$D^* B$	$D^* B^*$	$D_s B_s^*$	$D_s^* B_s$	$D_s^* B_s^*$
DB^*	$V_\sigma^d + \frac{3}{2}V_\rho^d + \frac{1}{2}V_\omega^d$	$\frac{3}{2}V_\pi^f + \frac{1}{6}V_\eta^f + \frac{3}{2}V_\rho^f + \frac{1}{2}V_\omega^f$	$V_\sigma^c + \frac{3}{2}V_\pi^c + \frac{1}{6}V_\eta^c + \frac{3}{2}V_\rho^c + \frac{1}{2}V_\omega^c$	$\sqrt{2}V_{K^*}^d$	$\sqrt{2}V_{K^*}^d$	$\sqrt{2}V_{K^*}^f + \sqrt{2}V_K^f$
$D^* B$	$\frac{3}{2}V_\pi^e + \frac{1}{6}V_\eta^e + \frac{3}{2}V_\rho^e + \frac{1}{2}V_\omega^e$	$\frac{3}{2}V_\pi^g + \frac{1}{6}V_\eta^g + \frac{3}{2}V_\rho^g + \frac{1}{2}V_\omega^g$	$\sqrt{2}V_{K^*}^e + \sqrt{2}V_K^e$	$\sqrt{2}V_{K^*}^g + \sqrt{2}V_K^g$		
$D^* B^*$		$V_\sigma^c + \frac{3}{2}V_\pi^c + \frac{1}{6}V_\eta^c + \frac{3}{2}V_\rho^c + \frac{1}{2}V_\omega^c$	$\sqrt{2}V_{K^*}^f + \sqrt{2}V_K^f$	$\sqrt{2}V_{K^*}^c + \sqrt{2}V_K^c$		
$D_s B_s^*$			$V_\sigma^d + V_\phi^d + \frac{2}{3}V_\eta^e + V_\phi^e$	$\frac{2}{3}V_\eta^f + V_\phi^f$		
$D_s^* B_s$				$\frac{2}{3}V_\eta^g + V_\phi^g$		
$D_s^* B_s^*$				$V_\sigma^c + \frac{2}{3}V_\eta^c + V_\phi^c$		
$I(J^{PC}) = 0(2^+)$	$D^* B^*$	$D_s^* B_s^*$				
$D^* B^*$	$V_\sigma^c + \frac{3}{2}V_\pi^c + \frac{1}{6}V_\eta^c + \frac{3}{2}V_\rho^c + \frac{1}{2}V_\omega^c$	$\sqrt{2}V_{K^*}^c + \sqrt{2}V_K^c$				
$D_s^* B_s^*$		$V_\sigma^c + \frac{2}{3}V_\eta^c + V_\phi^c$				
$I(J^{PC}) = 1(0^+)$	DB	$D^* B^*$				
DB	$V_\sigma^d - \frac{1}{2}V_\rho^d + \frac{1}{2}V_\omega^d$	$\frac{1}{6}V_\eta^b - \frac{1}{2} - \frac{1}{2}V_\rho^b + \frac{1}{2}V_\omega^b$				
$D^* B^*$		$V_\sigma^c - \frac{1}{2}V_\pi^c + \frac{1}{6}V_\eta^c - \frac{1}{2}V_\rho^c + \frac{1}{2}V_\omega^c$				
$I(J^{PC}) = 1(1^+)$	DB^*	$D^* B$	$D^* B^*$			
DB^*	$V_\sigma^d - \frac{1}{2}V_\rho^d + \frac{1}{2}V_\omega^d$	$\frac{3}{2}V_\pi^f + \frac{1}{6}V_\eta^f + \frac{3}{2}V_\rho^f + \frac{1}{2}V_\omega^f$	$-\frac{1}{2}V_\pi^f + \frac{1}{6}V_\eta^f - \frac{1}{2}V_\rho^f + \frac{1}{2}V_\omega^f$			
$D^* B$		$V_\sigma^d - \frac{1}{2}V_\rho^d + \frac{1}{2}V_\omega^d$	$-\frac{1}{2}V_\pi^f + \frac{1}{6}V_\eta^f - \frac{1}{2}V_\rho^f + \frac{1}{2}V_\omega^f$			
$D^* B^*$			$V_\sigma^c - \frac{1}{2}V_\pi^c + \frac{1}{6}V_\eta^c - \frac{1}{2}V_\rho^c + \frac{1}{2}V_\omega^c$			
$I(J^{PC}) = 1(2^+)$	$D^* B^*$					
$D^* B^*$	$V_\sigma^c - \frac{1}{2}V_\pi^c + \frac{1}{6}V_\eta^c - \frac{1}{2}V_\rho^c + \frac{1}{2}V_\omega^c$					

TABLE II: The relevant parameters adopted in this work.

Parameters	Value
g_V	5.800
g	0.590
g_s	2.820
β	0.900
f_π	0.132(GeV)
λ	0.560(GeV ⁻¹)

metry, there should exist exotic hadron states that correspond to the partners of the charmonium-like and bottomonium-like states in bottom-charmed sector. Therefore, we first investigate the $I(J^P) = 1(1^+) DB^*/D^*B/D^*B^*$ channel, which will also help us determine the cutoff value within a phenomenologically reasonable range.

For the $I(J^P) = 1(1^+) DB^*/D^*B/D^*B^*$ channel, no pole is found when the cutoff Λ is varied from 800 to 1300 MeV. However, at $\Lambda = 1400$ MeV, a narrow resonance emerges near the D^*B threshold, predominantly composed of the $D^*B(^3S_1)$ state. When the cutoff is further increased to 1450 MeV, a resonance with a complex energy of $E - i\Gamma/2 = 7333 - 7i$ MeV appears below the D^*B^* threshold. This resonance is primarily dominated by the $D^*B(^3S_1)$ channel, with a composition of

approximately 96%, and can be considered a promising partner of both the $T_{c\bar{c}1}(4020)$ and $T_{b\bar{b}1}(10650)$ states. As the cutoff increases to around 1500 MeV, a loosely bound state with a predicted mass of 7192 MeV is observed, which could be regarded as a counterpart to the $T_{c\bar{c}1}(3900)$ and $T_{b\bar{b}1}(10610)$ states. It is worth noting that, for a similar cutoff value, previous studies only identified bound states due to the consideration of single-channel interactions [61]. This highlights the significant role of coupled-channel effects in molecular state formation. In Figure 2, we present the complex energy eigenvalues for the $I(J^P) = 1(1^+)$ system at $\Lambda = 1500$ MeV, with the scaling angle θ varying from 15° to 25° . Also, we plot the variations of complex energies for these two predicted resonances with θ in Figure 3, where one can find that the numerical errors caused by the θ are tiny and rapidly converge with increasing θ . The corresponding numerical results are summarized in Table III and Figure 4(e). For the three predicted exotic states, the root-mean-square radius (r_{RMS}) is found to be consistent with typical hadronic molecules, such as the deuteron. Therefore, a cutoff range of 1200 ~ 1500 MeV is adopted to investigate other $D_{(s)}^{(*)}B_{(s)}^{(*)}$ systems. The corresponding numerical results for these systems, depending on the cutoff parameter Λ , are presented in Figure 4.

For the $I(J^P) = 1(0^+) DB/D^*B^*$ systems, a loosely bound state is predicted when the cutoff Λ is within the range of

TABLE III: The molecular states for $I(J^P) = 1(1^+)$ system. The numbers in the bracket are the components proportion of $DB^* + h.c.$, $D^*B + h.c.$, and D^*B^* channels.

$\Lambda(\text{MeV})$	$E(\text{MeV})$	$r_{\text{RMS}}(\text{fm})$	$(DB^*(^3S_1))$	$DB^*(^3D_1)$	$D^*B(^3S_1)$	$D^*B(^3D_1)$	$D^*B^*(^3S_1)$	$D^*B^*(^3D_1)$	$D^*B^*(^5D_1)$
1400	$7287.71 - 0.36i$	$3.79 + 1.76i$	(0.05)	0.27	97.88	0.01	1.62	0.03	0.14)
1450	$7287.07 - 0.53i$	$2.87 + 1.34i$	(0.07)	0.45	96.08	0.01	3.13	0.05	0.21)
	$7333.22 - 7.36i$	$2.62 + 1.22i$	(0.66)	0.09	3.01	0.15	95.67	0.40	0.02)
1500	$7286.03 - 0.67i$	$2.10 + 0.97i$	(0.07)	0.65	93.64	0.02	5.28	0.05	0.29)
	$7332.50 - 9.68i$	$2.13 + 0.99i$	(0.90)	0.11	4.30	0.19	94.00	0.48	0.02)
	$7191.81 - 0.00i$	$3.86 + 0.00i$	(99.54)	0.00	0.10	0.07	0.22	0.01	0.06)

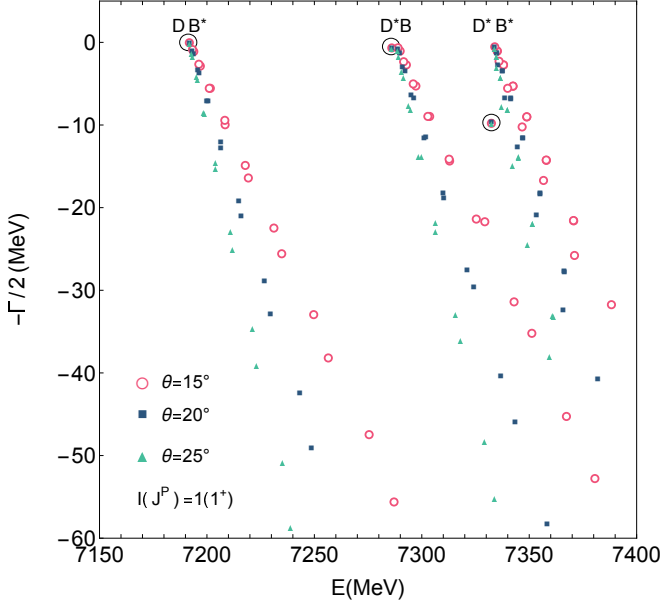


FIG. 2: The complex energy eigenvalues of $I(J^P) = 1(1^+)$ system with varying the angle θ from $15^\circ \sim 25^\circ$.

1400 ~ 1500 MeV. In this region, the root-mean-square radius r_{RMS} decreases from 4 to 2 fm, suggesting that it can be considered a promising molecular state candidate. However, for the D^*B^* system with spin-parity $I(J^P) = 1(2^+)$, no structure is observed in the complex energy plane when the cutoff is set to 1200 ~ 1500 MeV. It is important to note that the $I(J^P) = 1(2^+)$ system consists solely of the D^*B^* channel, where the attractive interaction is not strong enough to form a bound state compared to other isospin-vector systems. Nevertheless, by increasing the cutoff to approximately 2500 MeV, one may explore the possibility of a bound state.

B. Isospin scalar systems

Except for isospin vector systems, we also have isospin scalar systems for $D_{(s)}^{(*)}B_{(s)}^{(*)}$. Unlike the $I = 1$ systems, the $I = 0$ case allows for more coupled channels. As shown in Figure 4(a), we investigate the coupled-channel system

$DB/D^*B^*/D_sB_s/D_s^*B_s^*$ with spin-parity $I(J^P) = 0(0^+)$. A narrow resonance, predominantly composed of $D^*B^*(^1S_0)$ (59%), $D^*B^*(^1D_0)$ (8%), and $D_sB_s(^1S_0)$ (29%), appears near the D_sB_s threshold with a complex energy of $E - i\Gamma/2 = 7332 - 0.5i$ MeV when the cutoff value is set to $\Lambda = 1200$ MeV. By increasing the cutoff, a bound state solution emerges below the DB threshold, while the resonance evolves to $7387 - 0.3i$ MeV. Both states can be considered candidates for exotic hadronic states. Additionally, we identify a pole near the $D_s^*B_s^*$ threshold with a narrow width.

For the $I(J^P) = 0(1^+)$ channel, the dependence of the system on the cutoff is illustrated in Figure 4(b). When the cutoff is within the range 1200 ~ 1300 MeV, two poles are excluded, as their corresponding r_{RMS} values do not support a molecular interpretation. Interestingly, a cutoff-sensitive resonant state located below the D^*B threshold evolves into a bound state when the cutoff is increased to 1280 MeV. However, due to its relatively small r_{RMS} when Λ varies between 1300 and 1500 MeV, it is not considered a good molecular state candidate in the present work. Meanwhile, for the pole located below the $D_sB_s^*$ threshold, the complex energy $E - i\Gamma/2$ shifts from $7374 - 5i$ MeV to $7322 - 4i$ MeV as the cutoff increases from 1200 to 1500 MeV. When the cutoff further increases to 1320 MeV, a resonance with energy $7323 - 4i$ MeV, predominantly composed of the $D^*B^*(^3S_1)$ component, is obtained and can be interpreted as a possible partner of the X(4014) particle.

Finally, for the $I(J^P) = 0(2^+)$ $D^*B^*/D_s^*B_s^*$ system, a deeply bound state is observed at $\Lambda = 1200$ MeV. However, its r_{RMS} value indicates that it cannot be regarded as a molecular state. When the cutoff is increased to approximately $\Lambda = 1400$ MeV, a resonance with a predicted energy of $E - i\Gamma/2 = 7530 - 5i$ MeV appears near the $D_s^*B_s^*$ threshold. This state is predominantly composed of $D_s^*B_s^*(^3S_2)$ (94%) and can be suggested as a promising molecular state according to our analysis.

C. Further discussion

According to our calculations, owing to the presence of more allowed channels in the present work, both bound states and resonances are obtained for the $I = 0$ and $I = 1$ $D_{(s)}^{(*)}B_{(s)}^{(*)}$ systems, while only bound states are obtained for hidden bot-

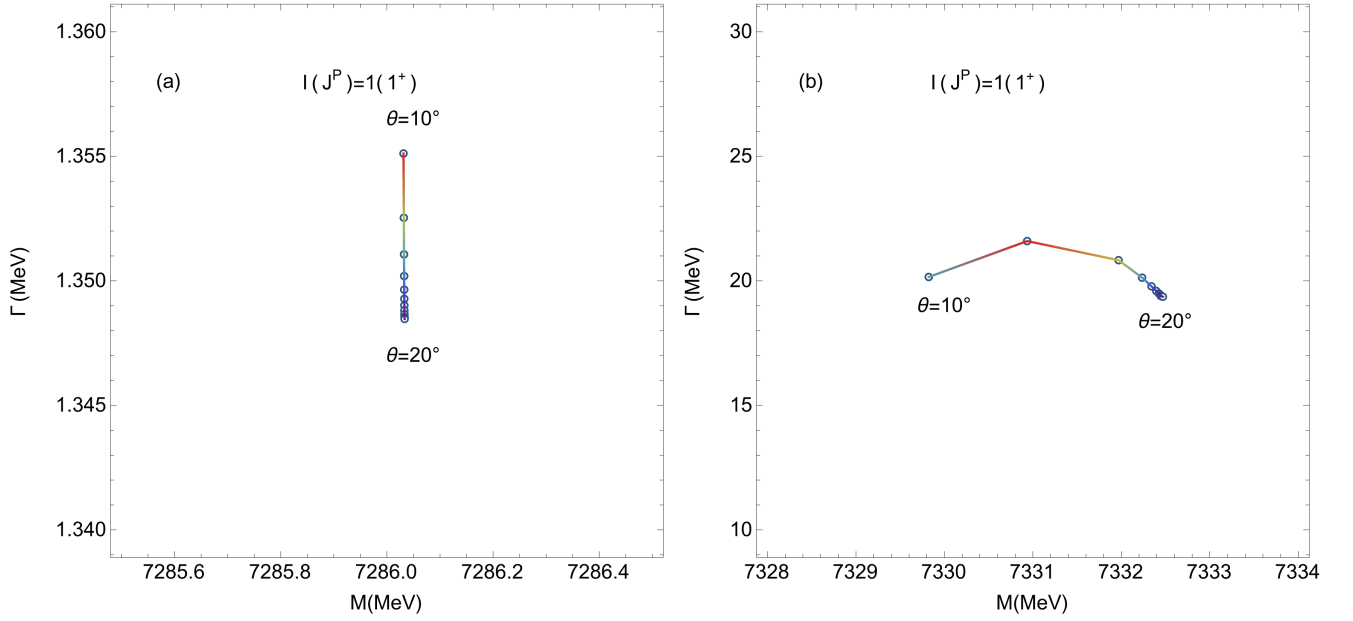


FIG. 3: The variations of complex energies for the two predicted $1(1)^+$ resonances with θ .

TABLE IV: The summary of our predictions for $D_{(s)}^{(*)}B_{(s)}^{(*)}$ systems with cutoff Λ in a range of 1300 ~ 1500 MeV. Here, the “-” means nonexistence, “✓”(“×”) represents that the corresponding state may (may not) form a molecular state.

$I(J^{PC})$	Mass(MeV)	Width(MeV)	r_{RMS} (fm)	Status	Selected decay mode
$0(0^+)$	7326.00 ~ 7277.68	0.76 ~ 0.82	$1.26 + 0.46i \sim 0.62 + 0.22i$	✓	$B_c\eta^{(\prime)}/B_c^*\omega/DB$
	7529.53 ~ 7529.21	6.62 ~ 7.04	$4.22 + 1.53i \sim 3.60 + 1.30i$	✓	$B_c\eta^{(\prime)}/B_c^*\phi/D_s^{(*)}B_s^{(*)}$
	7146.74 ~ 7145.49	—	$3.53 \sim 2.60$	✓	$B_c\eta^{(\prime)}/B_c^*\omega$
$0(1^+)$	7330.21 ~ 7251.60	25.14 ~ 23.42	$1.82 + 0.95i \sim 0.69 + 0.39i$	✓	$B_c\omega/B_c^*\eta^{(\prime)}/DB^*/D^*B$
	7361.89 ~ 7322.25	7.60 ~ 8.52	$0.90 + 0.52i \sim 0.72 + 0.41i$	×	—
	7182.86 ~ 7049.72	—	$1.00 \sim 0.48$	×	—
$0(2^+)$	7214.52 ~ 7079.97	—	$0.52 \sim 0.42$	×	—
	7530.29 ~ 7527.80	9.74 ~ 17.24	$3.07 + 0.54i \sim 1.90 + 0.51i$	✓	$B_c\phi/B_c^*\phi/D_s^{(*)}B_s^{(*)}$
$1(0^+)$	7146.69 ~ 7145.31	—	$4.33 \sim 2.46$	✓	$B_c\pi/B_c^*\rho$
$1(1^+)$	7288.05 ~ 7286.03	0.58 ~ 1.34	$4.50 + 1.20i \sim 2.07 + 0.55i$	✓	$B_c\rho/B_c^*\pi/DB^*$
	7333.25 ~ 7332.39	14.92 ~ 19.6	$2.06 + 0.55 \sim 1.86 + 0.50i$	✓	$B_c\rho/B_c^*\pi/DB^*/D^*B$
	7191.94 ~ 7191.83	—	$4.47 \sim 4.19$	✓	$B_c\rho/B_c^*\pi$
$1(2^+)$	—	—	—	×	—

tom molecular tetraquark state in $I = 1$ system [63]. It means that the coupled channels play crucial roles in production of molecule. For instance, when considering the single channel DB^* or D^*B with $I(J^P) = 1(1^+)$ case, we do not obtain any pole at cutoff in a range of 800 ~ 1500 MeV since the potential for them is too weak to form a molecule. However, if only single channel $1(1^+)D^*B^*$ is considered, a bound state is revealed at cutoff around 1300 MeV, which is consistent well with Ref. [74]. Meanwhile, if we discard the contributions from the D -wave, we also obtain bound and resonant states with a large cutoff parameter, which demonstrates that

the coupled channel effect plays a dominant role in the formation of resonant states and with the main contributions coming from S -wave.

It is also noteworthy that the root mean square (r_{RMS}) of the predicted resonances is a complex number. In such case, one can adopt the interpretation scheme proposed by T. Berggren, which extends the definition of expectation values beyond bound states to include resonant states [85]. According to this framework, the real part of r_{RMS} corresponds to the conventional physical expectation value, characterizing the spatial extent of the resonance, while the imaginary part provides

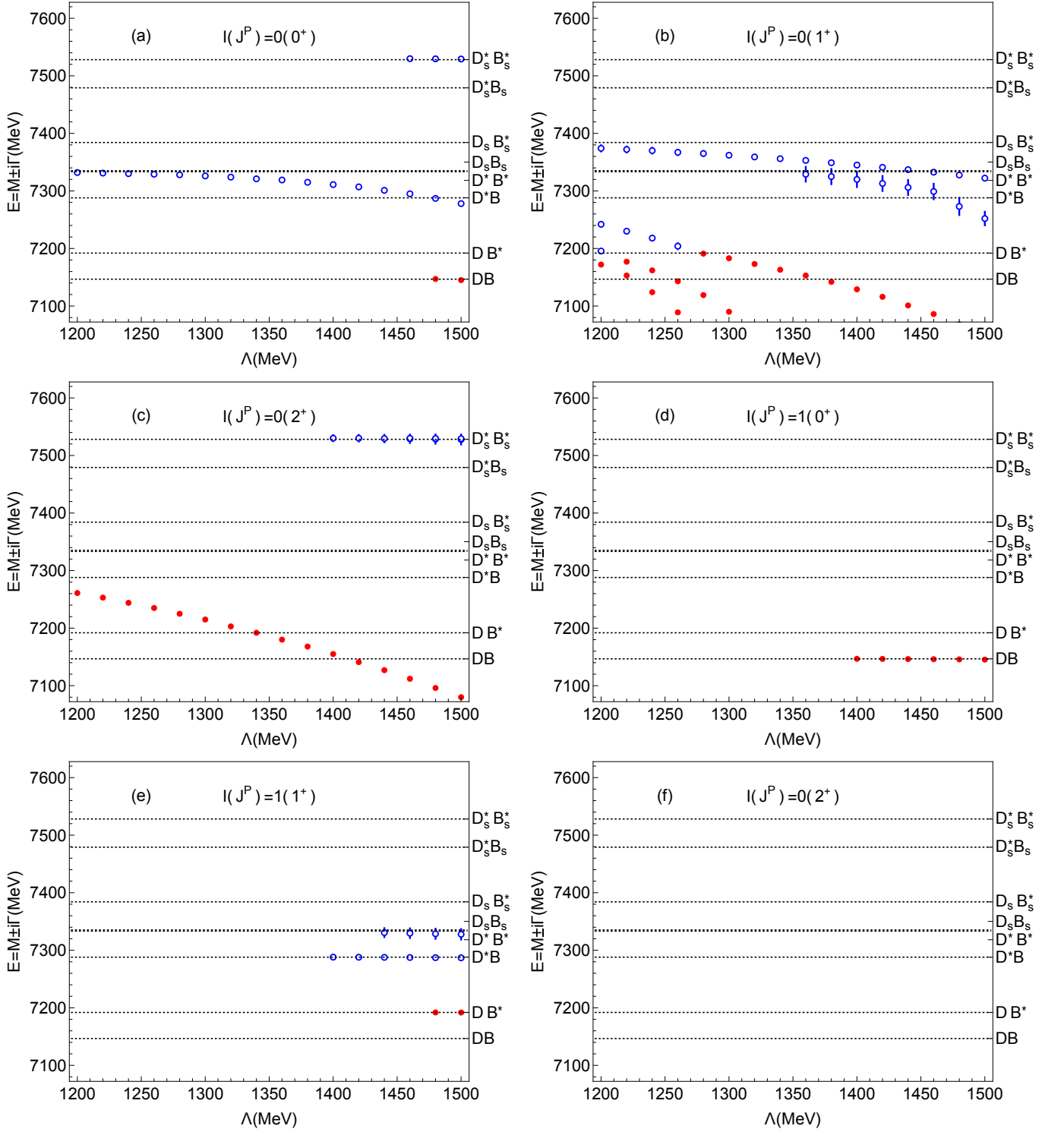


FIG. 4: The Λ dependence for the $D_{(s)}^{(*)}B_{(s)}^{(*)}$ systems. The blue open circles with bars correspond to the resonances, and the bars represent the total widths for resonances.

a measure of the uncertainty associated with its observation, reflecting the finite lifetime and decay properties of the state. Numerical calculations of r^2 further support this generalized interpretation [86, 87], showing that complex expectation values naturally emerge in resonant systems.

Moreover, we prefer to collect the final results of $D_{(s)}^{(*)}B_{(s)}^{(*)}$ systems in Table IV, where we predict nine exotic particles. As plotted in figure 4(b) and Table IV, for $I(J^P) = 0(1^+)$ system, we predict three exotic states near DB^* , D^*B , and D^*B^* thresholds, respectively, which may be regarded as good

molecular state and be counterparts to the exotic states already observed in both the charm and bottom sectors. Also, for $I(J^P) = 1(1^+)$ system, three molecular states are found below their thresholds, respectively, which are shown in figure 4(e) and Table IV. However, whether the $T_{bb1}(10610)$ and $T_{bb1}(10650)$ are located above or below the corresponding thresholds is still an open question. For the bottom-charmed molecular tetraquark states, they may also encounter the same question, thus, the further theoretical studies and experimental explorations are needed. Finally, according to the masses and quantum numbers, we collect some possible decay modes of these predicted particles in Table IV. It can be evident that the B_c/B_c^* plus light mesons are the ideal final states to search for the bound states, while the $D_{(s)}^{(*)}B_{(s)}^{(*)}$ channels are suitable for the resonances. We highly recommend that the future experiments could hunt for these bottom-charmed exotic particles in the future.

IV. SUMMARY

In this work, we investigate the $D_{(s)}^{(*)}B_{(s)}^{(*)}$ systems from a coupled-channel perspective by adopting the OBE model. By utilizing the Gaussian expansion method and complex scaling method, the coupled-channel Schrödinger equation is solved and nine exotic hadronic states are picked out. Firstly, we study the $D_{(s)}^{(*)}B_{(s)}^{(*)}$ system with $I(J^P) = 1(1^+)$, and some

poles are obtained and labeled as T_{cb1} , which may be regarded as partners of the discovered exotic states T_{cc1} and T_{bb1} . Then, the various $D_{(s)}^{(*)}B_{(s)}^{(*)}$ combinations with different quantum numbers are studied to search for possible bound states and resonances. For $I(J^P) = 0(1^+)$ system, we also predict one molecular state near the D^*B^* threshold. We hope our present calculations provide helpful information and strongly recommend that future experiments search for these exotic particles.

ACKNOWLEDGMENTS

We would like to thank Dian-Yong Chen for useful discussions. The work of X.-N. X. and Q. F. Song is supported by the National Natural Science Foundation of China under Grants No. 12275364. Q.-F. Lü is supported by the Natural Science Foundation of Hunan Province under Grant No. 2023JJ40421, the Scientific Research Foundation of Hunan Provincial Education Department under Grant No. 24B0063, and the Youth Talent Support Program of Hunan Normal University under Grant No. 2024QNTJ14. Wei Liang is supported by the Fundamental Research Funds for the Central Universities of Central South University under Grants No. 1053320214315 and No. 2022ZZTS0169, the Postgraduate Scientific Research Innovation Project of Hunan Province under Grant No. CX20220255.

-
- [1] S. K. Choi *et al.* [Belle], Phys. Rev. Lett. **91**, 262001 (2003).
 - [2] M. Ablikim *et al.* [BESIII], Phys. Rev. Lett. **110**, 252001 (2013).
 - [3] Z. Q. Liu *et al.* [Belle], Phys. Rev. Lett. **110**, 252002 (2013) [erratum: Phys. Rev. Lett. **111**, 019901 (2013)].
 - [4] M. Ablikim *et al.* [BESIII], Phys. Rev. Lett. **111**, No.24, 242001 (2013).
 - [5] X. L. Wang *et al.* [Belle], Phys. Rev. D **105**, No.11, 112011 (2022).
 - [6] A. Bondar *et al.* [Belle], Phys. Rev. Lett. **108**, 122001 (2012).
 - [7] H. X. Chen, W. Chen, X. Liu and S. L. Zhu, Phys. Rept. **639**, 1-121 (2016).
 - [8] A. Hosaka, T. Iijima, K. Miyabayashi, Y. Sakai and S. Yasui, PTEP **2016**, 062C01 (2016).
 - [9] R. F. Lebed, R. E. Mitchell and E. S. Swanson, Prog. Part. Nucl. Phys. **93**, 143 (2017).
 - [10] A. Esposito, A. Pilloni and A. D. Polosa, Phys. Rept. **668**, 1 (2017).
 - [11] F. K. Guo, C. Hanhart, U. G. Meißner, Q. Wang, Q. Zhao and B. S. Zou, Rev. Mod. Phys. **90**, 015004 (2018).
 - [12] M. Karliner, J. L. Rosner and T. Skwarnicki, Ann. Rev. Nucl. Part. Sci. **68**, 17 (2018).
 - [13] Y. Dong, A. Faessler and V. E. Lyubovitskij, Prog. Part. Nucl. Phys. **94**, 282 (2017).
 - [14] S. L. Olsen, T. Skwarnicki and D. Zieminska, Rev. Mod. Phys. **90**, 015003 (2018).
 - [15] A. Ali, J. S. Lange and S. Stone, Prog. Part. Nucl. Phys. **97**, 123 (2017).
 - [16] Y. R. Liu, H. X. Chen, W. Chen, X. Liu and S. L. Zhu, Prog. Part. Nucl. Phys. **107**, 237 (2019).
 - [17] N. Brambilla, S. Eidelman, C. Hanhart, A. Nefediev, C. P. Shen, C. E. Thomas, A. Vairo and C. Z. Yuan, Phys. Rept. **873**, 1 (2020).
 - [18] M. Y. Barabanov, M. A. Bedolla, W. K. Brooks, G. D. Cates, C. Chen, Y. Chen, E. Cisbani, M. Ding, G. Eichmann and R. Ent, *et al.*, Prog. Part. Nucl. Phys. **116**, 103835 (2021).
 - [19] P. Bicudo, Phys. Rept. **1039**, 1-49 (2023).
 - [20] H. X. Chen, W. Chen, X. Liu, Y. R. Liu and S. L. Zhu, Rept. Prog. Phys. **86**, no.2, 026201 (2023).
 - [21] M. Mai, U. G. Meißner and C. Urbach, Phys. Rept. **1001**, 1-66 (2023).
 - [22] M. Z. Liu, Y. W. Pan, Z. W. Liu, T. W. Wu, J. X. Lu and L. S. Geng, Phys. Rept. **1108**, 1-108 (2025).
 - [23] Z. G. Wang, [arXiv:2502.11351 [hep-ph]].
 - [24] F. Abe *et al.* [CDF], Phys. Rev. D **58**, 112004 (1998).
 - [25] R. Aaij *et al.* [LHCb], Phys. Rev. Lett. **109**, 232001 (2012).
 - [26] V. M. Abazov *et al.* [D0], Phys. Rev. Lett. **101**, 012001 (2008).
 - [27] S. Navas *et al.* [Particle Data Group], Phys. Rev. D **110**, no.3, 030001 (2024).
 - [28] A. M. Sirunyan *et al.* [CMS], Phys. Rev. Lett. **122**, no.13, 132001 (2019).
 - [29] R. Aaij *et al.* [LHCb], Phys. Rev. Lett. **122**, no.23, 232001 (2019).
 - [30] S. Godfrey and N. Isgur, Phys. Rev. D **32**, 189-231 (1985).
 - [31] W. k. Kwong and J. L. Rosner, Phys. Rev. D **44**, 212-219 (1991).
 - [32] E. J. Eichten and C. Quigg, Phys. Rev. D **49**, 5845-5856 (1994).
 - [33] J. Zeng, J. W. Van Orden and W. Roberts, Phys. Rev. D **52**,

- 5229-5241 (1995).
- [34] S. N. Gupta and J. M. Johnson, Phys. Rev. D **53**, 312-314 (1996).
 - [35] L. P. Fulcher, Phys. Rev. D **60**, 074006 (1999).
 - [36] D. Ebert, R. N. Faustov and V. O. Galkin, Phys. Rev. D **67**, 014027 (2003).
 - [37] S. M. Ikhdaïr and R. Sever, Int. J. Mod. Phys. A **19**, 1771-1792 (2004).
 - [38] S. Godfrey, Phys. Rev. D **70**, 054017 (2004).
 - [39] S. M. Ikhdaïr and R. Sever, Int. J. Mod. Phys. A **20**, 4035-4054 (2005).
 - [40] S. M. Ikhdaïr and R. Sever, Int. J. Mod. Phys. A **20**, 6509-6531 (2005).
 - [41] N. R. Soni, B. R. Joshi, R. P. Shah, H. R. Chauhan and J. N. Pandya, Eur. Phys. J. C **78**, no.7, 592 (2018).
 - [42] E. J. Eichten and C. Quigg, Phys. Rev. D **99**, no.5, 054025 (2019).
 - [43] Q. Li, M. S. Liu, L. S. Lu, Q. F. Lü, L. C. Gui and X. H. Zhong, Phys. Rev. D **99**, no.9, 096020 (2019).
 - [44] I. F. Allison *et al.* [HPQCD, Fermilab Lattice and UKQCD], Phys. Rev. Lett. **94**, 172001 (2005).
 - [45] R. J. Dowdall, C. T. H. Davies, T. C. Hammant and R. R. Horgan, Phys. Rev. D **86**, 094510 (2012).
 - [46] N. Mathur, M. Padmanath and S. Mondal, Phys. Rev. Lett. **121**, no.20, 202002 (2018).
 - [47] Z. G. Wang, Eur. Phys. J. A **49**, 131 (2013).
 - [48] S. S. Gershtein, V. V. Kiselev, A. K. Likhoded and A. V. Tkabladze, Phys. Rev. D **51**, 3613-3627 (1995).
 - [49] J. Wu, X. Liu, Y. R. Liu and S. L. Zhu, Phys. Rev. D **99**, no.1, 014037 (2019).
 - [50] U. Özdem, Eur. Phys. J. Plus **140**, no.2, 105 (2025).
 - [51] U. Özdem, Phys. Lett. B **838**, 137750 (2023).
 - [52] R. M. Albuquerque, X. Liu and M. Nielsen, Phys. Lett. B **718**, 492-498 (2012).
 - [53] J. R. Zhang and M. Q. Huang, Commun. Theor. Phys. **54**, 1075-1090 (2010).
 - [54] W. Chen, T. G. Steele and S. L. Zhu, Phys. Rev. D **89**, no.5, 054037 (2014).
 - [55] S. S. Agaev, K. Azizi and H. Sundu, Phys. Rev. D **95**, no.3, 034008 (2017).
 - [56] S. S. Agaev, K. Azizi and H. Sundu, Eur. Phys. J. C **77**, no.5, 321 (2017).
 - [57] Q. N. Wang and W. Chen, Eur. Phys. J. C **80**, no.5, 389 (2020).
 - [58] J. R. Zhang and M. Q. Huang, Phys. Rev. D **80**, 056004 (2009).
 - [59] Z. Y. Wang and Z. F. Sun, Eur. Phys. J. C **83**, no.12, 1106 (2023).
 - [60] S. Sakai, L. Roca and E. Oset, Phys. Rev. D **96**, no.5, 054023 (2017).
 - [61] Z. F. Sun, X. Liu, M. Nielsen and S. L. Zhu, Phys. Rev. D **85**, 094008 (2012).
 - [62] F. L. Wang, S. Q. Luo and X. Liu, Phys. Rev. D **107**, no.11, 114017 (2023).
 - [63] Q. F. Song, Q. F. Lü, D. Y. Chen and Y. B. Dong, Phys. Rev. D **110**, no.7, 074038 (2024).
 - [64] Q. F. Song, Q. F. Lü and X. Xiong, [arXiv:2501.01077 [hep-ph]].
 - [65] E. Hiyama, Y. Kino and M. Kamimura, Prog. Part. Nucl. Phys. **51**, 223-307 (2003).
 - [66] E. Hiyama and M. Kamimura, Front. Phys. (Beijing) **13**, 132106 (2018).
 - [67] N. Moiseyev, Phys. Rept. **302**, No.5-6, 212-293 (1998).
 - [68] Y. K. Ho, Phys. Rept. **99**, No.1, 1-68 (1983).
 - [69] M. B. Wise, Phys. Rev. D **45**, No.7, R2188 (1992).
 - [70] T. M. Yan, H. Y. Cheng, C. Y. Cheung, G. L. Lin, Y. C. Lin and H. L. Yu, Phys. Rev. D **46**, 1148-1164 (1992) [erratum: Phys. Rev. D **55**, 5851 (1997)].
 - [71] G. Burdman and J. F. Donoghue, Phys. Lett. B **280**, 287-291 (1992).
 - [72] R. Casalbuoni, A. Deandrea, N. Di Bartolomeo, R. Gatto, F. Feruglio and G. Nardulli, Phys. Rept. **281**, 145 (1997).
 - [73] M. Bando, T. Kugo and K. Yamawaki, Phys. Rept. **164**, 217-314 (1988).
 - [74] Z.-F. Sun, J. He, X. Liu, Z.-G. Luo and S.-L. Zhu, Phys. Rev. D **84**, 054002 (2011).
 - [75] R. Chen and Q. Huang, Phys. Lett. B **846**, 138254 (2023).
 - [76] N. Li and S. L. Zhu, Phys. Rev. D **86**, 074022 (2012).
 - [77] C. Isola, M. Ladisa, G. Nardulli and P. Santorelli, Phys. Rev. D **68**, 114001 (2003).
 - [78] F. L. Wang and X. Liu, Phys. Rev. D **104**, 094030 (2021).
 - [79] F. L. Wang, R. Chen, Z. W. Liu and X. Liu, Phys. Rev. D **99**, No.5, 054021 (2019).
 - [80] R. Machleidt, K. Holinde and C. Elster, Phys. Rept. **149**, 1-89 (1987).
 - [81] M. Homma, T. Myo, and K. Katō, Prog. Theor. Phys. **97**, 561 (1997).
 - [82] Z. Y. Lin, J. B. Cheng, B. L. Huang and S. L. Zhu, Phys. Rev. D **108**, No.11, 114014 (2023).
 - [83] N. A. Tornqvist, Z. Phys. C **61**, 525-537 (1994).
 - [84] N. A. Tornqvist, Nuovo Cim. A **107**, 2471-2476 (1994) [arXiv:hep-ph/9310225 [hep-ph]].
 - [85] T. Berggren, Phys. Lett. B **33**, 547-549 (1970).
 - [86] B. Gyarmati, F. Krisztinkovics and T. Vertse, Phys. Lett. B **41**, 110-112 (1972).
 - [87] M. Homma, T. Myo, K. Katō, Prog., Theor. Phys. **97** (1997) 561.